Manganese oxide catalysts supported on TiO2, Al2O3, and SiO2: A comparison for low-temperature SCR of NO with NH3

4 AUTHORS, INCLUDING:

Panagiotis G Smirniotis
University of Cincinnati

146 PUBLICATIONS **5,231** CITATIONS

Robert G. Jenkins
University of Vermont

143 PUBLICATIONS **2,457** CITATIONS

KINETICS, CATALYSIS, AND REACTION ENGINEERING

Manganese Oxide Catalysts Supported on TiO$_2$, Al$_2$O$_3$, and SiO$_2$: A Comparison for Low-Temperature SCR of NO with NH$_3$

Panagiotis G. Smirniotis,*,† Pavani M. Sreekanth,† Donovan A. Peña,† and Robert G. Jenkins‡

Chemical and Materials Engineering Department, University of Cincinnati, Cincinnati, Ohio 45221-0012, and School of Engineering, The University of Vermont, Burlington, Vermont 05405-0156

A series of TiO$_2$-, Al$_2$O$_3$-, and SiO$_2$-supported manganese oxide catalysts were prepared, characterized, and catalytically tested for selective catalytic reduction (SCR) of NO with NH$_3$ in the presence of excess oxygen at low temperatures (373−523 K). Various commercial supports were used in this study to find out the influence of surface area, support nature (acidic, basic), and crystalline phase on SCR activity. XRD studies reveal the presence of anatase and rutile phases for titania supports and the existence of γ-alumina in the case of alumina support. Silica support was amorphous. No independent lines corresponding to the crystalline MnO$_2$ were observed on pure anatase and rutile samples. However, the presence of MnO$_2$ was confirmed on other supports by XRD. BET surface area values suggest that specific surface area of the supports was decreased after impregnating with MnO$_2$. The FT-IR and ammonia TPD studies indicate the presence of two types of acid sites on these catalysts, and the acidic strength of the catalysts is higher than the corresponding pure supports. XPS results revealed the presence of two types of manganese oxides, MnO$_2$ (642.4 eV) and Mn$_2$O$_3$ (641.2 eV), on all the samples. The SCR performance of the supported Mn catalysts decreased in the following order: TiO$_2$ (anatase, high surface area) > TiO$_2$ (rutile) > TiO$_2$ (anatase, rutile) > γ-Al$_2$O$_3$ > SiO$_2$ > TiO$_2$ (anatase, low surface area). Quantitative NO conversion with 100% N$_2$ selectivity was achieved at 393 K with Mn supported on TiO$_2$ (anatase). TiO$_2$-supported MnO$_2$ catalysts showed more promising SCR activity than Al$_2$O$_3$- or SiO$_2$-supported manganese oxide catalysts. Various characterization techniques suggest that Lewis acid sites, a high surface concentration of MnO$_2$, and redox properties are important in achieving high catalytic performance at low temperatures.

1. Introduction

Nitrogen oxides (NO$_x$, a mixture of approximately 95% NO and 5% NO$_2$) are troublesome pollutants that have detrimental effects on the environment and on human health.[1,2] This has resulted in strict environmental legislation and restrictive emission standards for nitrogen oxides. A popular commercial process to remove NO$_x$ from stationary sources such as oil- and coal-fired power plants is the selective catalytic reduction (SCR) of NO with NH$_3$ in the presence of excess oxygen. The most effective industrial catalyst for the SCR process is based on V$_2$O$_5$/TiO$_2$ (anatase) promoted with either WO$_3$ or MoO$_3$.[3−6] Because of the high operating temperatures required (>623 K) for this catalyst, it must be located upstream of the desulfurizer and/or particulate control device to avoid reheating the flue gas. However, this accelerates catalyst deactivation through exposure to high concentrations of SO$_2$ and particulate matter. Recently, efforts have been made to develop catalysts capable of operating in the low-temperature range of 353−523 K[7−10] so that the catalyst bed can be shifted downstream of the desulfurizer and/or particulate control device. More importantly, it will help eliminate the need to reheat the stack gas, resulting in a lower investment and also a thermally more efficient process.

Carbon-supported copper,[7,8] vanadium[9,11] and manganese[12] oxides, copper−nickel and vanadium oxides supported on titania and alumina monoliths,[13] amorphous chromia,[14] chromia supported on TiO$_2$,[15] and alumina-supported manganese oxide[16] show high activity for NO reduction with NH$_3$ at low temperatures. However, no efforts have been made to compare the SCR activity for transition metal oxides deposited on various supports. In our previous studies,[17,18] we demonstrated the exceptionally high activity of Mn-, Cu-, and Cr-supported TiO$_2$ catalysts for SCR of NO at low temperature (353−423 K). The 20 wt % Mn/TiO$_2$ catalyst was found to be extremely active, giving 100% NO conversion with 100% N$_2$ selectivity at 393 K.

In continuation of our earlier studies, this work compares MnO$_2$ deposited on various commercial supports such as TiO$_2$ (anatase and rutile), γ-Al$_2$O$_3$, and SiO$_2$ for low-temperature SCR of NO. The main goal of this work is to understand the effect of the nature of the support used on SCR activity and to understand the specific types of surface species responsible for the catalytic activity. For this purpose, a series of TiO$_2$-, Al$_2$O$_3$-, and SiO$_2$-supported manganese oxide catalysts were prepared by the wet impregnation method. The prepared catalysts were thoroughly characterized by XRD, temperature-programmed desorption (TPD), temperature-programmed reduction (TPR), in situ FT-IR, and X-ray photoelectron spectroscopy (XPS) techniques.

2. Experimental Section

2.1. Catalyst Preparation. Commercially available titania, alumina, and silica supports were obtained from various manufacturers. These sources include: Hombikat TiO$_2$ from

* To whom correspondence should be addressed. Tel.: (513) 556-1474. Fax: (513) 556-3473. E-mail: panagiotis.smirniotis@uc.edu.
† University of Cincinnati.
‡ University of Vermont.

Sachtleben Chemie (99% anatase), TiO_2 from Kemira (100% rutile), P25 TiO_2 from Degussa AG (80% anatase and 20% rutile), TiO_2 from Aldrich (100% anatase), γ-Al_2O_3 from Puralox, and high surface area SiO_2 from Aldrich. Manganese oxide was deposited on these supports using aqueous solutions of manganese nitrate by the solution impregnation method. In a typical synthesis, 50 mL of deionzied water was added to a 100-mL beaker containing 1 g of support. The mixture was heated to 343 K under continuous stirring. A measured quantity of nitrate precursor was then added to the solution, and the mixture was evaporated to dryness. The paste obtained was further dried overnight at 383 K. Catalysts were calcined at 673 K for 2 h in a flow of O_2 (4.0% oxygen in helium).

2.2. X-ray Diffraction. X-ray powder diffraction patterns have been recorded on a Siemens D500 diffractometer using a Cu Kα radiation source (wavelength 1.5406 Å). An aluminum holder was used to support the catalyst samples. The scanning range was 5−70° (2θ) with a step size of 0.05° and a step time of 1 s. The XRD phases present in the samples were identified with the help of JCPDS data files.

2.3. BET Surface Area and Pore Size Measurements. The specific surface areas of the supports and the catalysts were measured by nitrogen physisorption at liquid nitrogen temperature (77 K) by the BET method using a Micromeritics Gemini 2360 instrument. Pore size measurements of various supports were performed using a Micromeritics ASAP 2010 instrument. Prior to analysis, all samples were degassed in situ at 523 K under vacuum.

2.4. X-ray Photoelectron Spectroscopy. The XPS measurements were made on a Perkin-Elmer (model 5300) spectrometer using Mg Kα (1253.6 eV) radiation as the excitation source. The spectra were recorded in the fixed analyzer transmission mode with pass energies of 89.45 and 35.75 eV for recording survey and high-resolution spectra, respectively. The XPS analysis was done at room temperature and at pressures in the order of 10^{-7} Torr. Charging of the catalyst samples was corrected by setting the binding energy of the Ti $2p_{3/2}$ at 458.5 eV. Samples were degassed in a vacuum oven overnight before XPS measurements.

2.5. FT-IR Spectroscopy. The FT-IR analysis was performed on a Bio-Rad spectrophotometer (FTS-40) from 400 to 4000 cm^{-1}. The scans were collected at a scan speed of 5 kHz, resolution of 2.0, and an aperture opening of 2.0 cm^{-1}. Circular self-supporting wafers (8-mm diameter) of the catalysts were used for the study. Sixteen scans were collected and averaged for each temperature. The wafers were placed in a high-temperature cell with CaF_2 windows and purged with prepurified grade helium (30 mL min^{-1}) at 673 K for 2 h to remove impurities. Then, the samples were cooled to 323 K, and NH_3 (4.4 vol % in He) was introduced to the cell with a flow of 30 mL min^{-1} for 1 h at 323 K to ensure complete saturation of the sample. Physisorbed ammonia was removed by flushing the wafer with He for sufficient time at 373 K. Subsequently, the FT-IR spectra were recorded by desorbing NH_3 at 373, 423, 473, 573, 673, and 773 K.

2.6. Ammonia Temperature-Programmed Desorption. The TPD experiments were performed on a custom-made setup using 50 mg of catalyst. Prior to the experiments, the catalysts were pretreated at 773 K for 1 h in an ultrahigh pure He (30 mL min^{-1}) stream. The furnace temperature was lowered to 373 K, and the samples were then saturated with anhydrous NH_3 (4% in He) at a flow rate of 30 mL min^{-1} for 1 h. Physisorbed NH_3 was removed by flushing the catalyst with helium at 373 K for 3−5 h before starting the TPD experiments. The heating

Table 1. Physical Properties of the Different Supports Used in This Study[a]

support	commercial source	crystalline phase	BET surface area (m^2 g^{-1})	pore volume (cm^3 g^{-1})	pore diam (nm)
Hombikat TiO_2	Sachtleben Chemie	A	309	0.70	4.5
P-25 TiO_2	Degussa AG	A:R (80:20)	51	0.18	14.8
Aldrich TiO_2	Aldrich	A	9	0.03	13.1
Kemira TiO_2	Kemira	R	52	0.22	16.7
Puralox γ-Al_2O_3	Condea		205	0.71	9.2
Aldrich SiO_2	Aldrich		565	0.95	6.5

[a] A = Anatase; R = Rutile.

rate for the TPD measurements from 373 to 773 K was 5 K min^{-1}. A thermal conductivity detector was used for the continuous monitoring of the desorbed ammonia.

2.7. Temperature-Programmed Reduction. The temperature-programmed reduction experiments were carried out from 353 to 1223 K on a Micromeritics AutoChem 2910 instrument using 50 mg of calcined catalyst. Prior to the analysis, the catalysts were pretreated at 673 K for 2 h in ultrahigh pure helium (30 mL min^{-1}) stream. The TPR runs were carried out with a linear heating rate of 10 °C/min in a flow of 4% H_2 in argon with a flow rate of 25 mL min^{-1}. The hydrogen consumption was measured quantitatively by a thermal conductivity detector.

2.8. Apparatus and Catalytic Experiments. The SCR of NO at atmospheric pressure was carried out in a fixed bed ceramic alumina reactor (i.d. 6 mm) containing 0.1 g of catalyst (80−120 mesh). Oxygen (Wright Bros., 4.18% in He), ammonia (Matheson, 3.89% in He), and nitric oxide (Air Products, 2.0% in He) were used as received. The inlet concentrations of NO and NH_3 were 2000 ppm, whereas the O_2 concentration was 20 000 ppm (2.0 vol %) for runs performed at the space velocity 8000 h^{-1}. Experiments performed at the space velocity 50 000 h^{-1} had inlet concentrations of 400 ppm for NH_3 and NO, and oxygen remained constant at 2 vol %. A syringe pump was used to inject the water into the reactor. The reaction temperature was measured by a type K thermocouple inserted directly into the catalyst bed. Prior to the catalytic experiments, the catalyst was activated in situ by passing oxygen for 2 h at 673 K. The reactants and products were analyzed online using a Quadrapole mass spectrometer (MKS PPT-RGA) and a chemiluminescence detector (Eco Physics CLD 70S).

3. Results and Discussion

3.1. Physical Properties of the Supports and the Catalysts. The physical properties of various supports used in this study are presented in Table 1. Among the titania supports, Hombikat is purely anatase and the BET surface area is 309 m^2 g^{-1}, while Kemira TiO_2 consisted entirely of rutile and had a surface area of 52 m^2 g^{-1}. The TiO_2 supports discussed above were selected to study the influence of surface area and crystalline phase of TiO_2 on SCR activity. The other supports used are Puralox (Condea) γ-Al_2O_3 with a surface area of 205 m^2 g^{-1} and SiO_2 with a surface area of 565 m^2 g^{-1}.

The physical characteristics of the supported MnO_2 catalysts are presented in Table 2. Specific surface area of the supports was decreased after impregnating with MnO_2. Decrease in surface area is more prominent in the case of Hombikat TiO_2 and SiO_2 supports. This is mainly due to the plugging of the micropores of the support materials by the impregnated manganese oxide. However, the surface area of Aldrich TiO_2 is

Table 2. Surface Area and Total Acidity Values of the Supported MnO$_2$ Catalysts Calcined at 673 K for 2 h

supports	BET surface area (m^2 g^{-1})		total acidity μmol g^{-1}
	support	catalyst	
TiO$_2$[a]	309	204	23.2
TiO$_2$[b]	52	52	15.2
TiO$_2$[c]	9	14	1.1
TiO$_2$[d]	52	50	11.0
Al$_2$O$_3$[e]	205	180	30.9
SiO$_2$[c]	565	421	5.9

[a] Hombikat. [b] Degussa P25. [c] Aldrich. [d] Kemira. [e] Puralox.
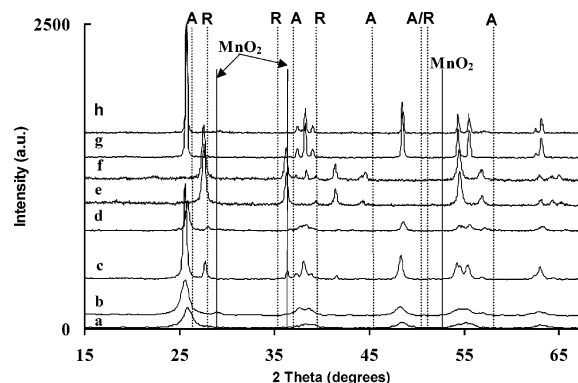
Figure 1. XRD diffractograms for (a) TiO$_2$ (Hombikat), (b) 20 wt % Mn/TiO$_2$ (Hombikat), (c) TiO$_2$ (Degussa P-25), (d) 20 wt % Mn/TiO$_2$ (Degussa P-25), (e) TiO$_2$ (Kemira), (f) 20 wt % Mn/TiO$_2$ (Kemira), (g) TiO$_2$ (Aldrich), and (h) 20 wt % Mn/ TiO$_2$ (Aldrich) [A = Anatase, R = Rutile].
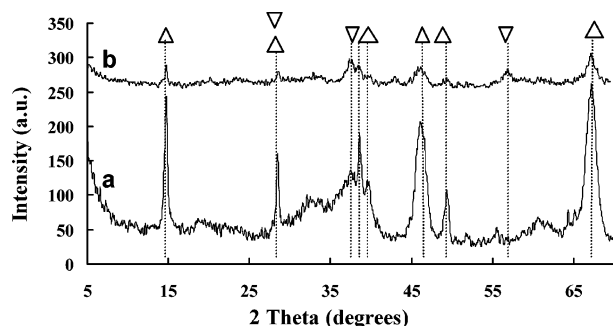
Figure 2. XRD diffractograms for (a) γ-Al$_2$O$_3$ (Puralox) and (b) 20 wt % Mn/γ-Al$_2$O$_3$ (Puralox) [$\triangle$ = γ-Al$_2$O$_3$, $\triangledown$ = MnO$_2$].

increased after impregnating with MnO$_2$. The total acidity values of various catalysts are depicted in Table 2. In the case of titania-supported manganese oxide catalysts, total acidity increased with an increase in surface area of the support. The SiO$_2$-supported catalyst possesses low acidity, regardless of the high surface area of the SiO$_2$ support (565 m^2 g^{-1}). The Mn/γ-Al$_2$O$_3$ catalyst showed the highest acidity because of the acidic nature of the support.

3.2. X-ray Diffraction. XRD patterns of the pure supports and the catalysts are presented in Figures 1−3. XRD patterns of various commercial TiO$_2$ supports and their corresponding MnO$_2$ impregnated catalysts are shown in Figure 1. Pure anatase phase was observed for Hombikat TiO$_2$ and only rutile modification was seen in the case of Kemira TiO$_2$. The high surface area Hombikat TiO$_2$ showed broad diffraction bands indicating the amorphous nature of the sample. No independent lines corresponding to the crystalline MnO$_2$ were observed on these samples. It indicates that incorporated manganese oxide dispersed homogeneously on titania supports and is in amorphous or poorly crystalline state. The XRD patterns of γ-Al$_2$O$_3$
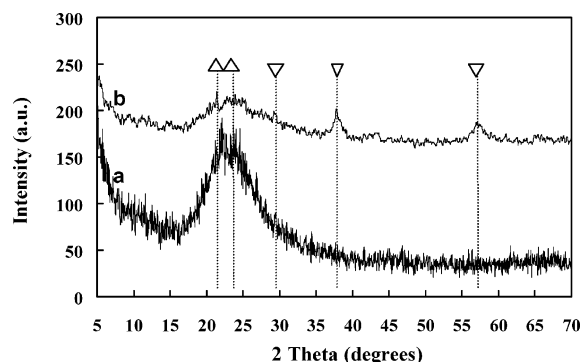
Figure 3. XRD diffractograms of (a) SiO$_2$ (Aldrich) and (b) 20 wt % Mn/SiO$_2$ (Aldrich) [$\triangle$ = SiO$_2$, $\triangledown$ = MnO$_2$].
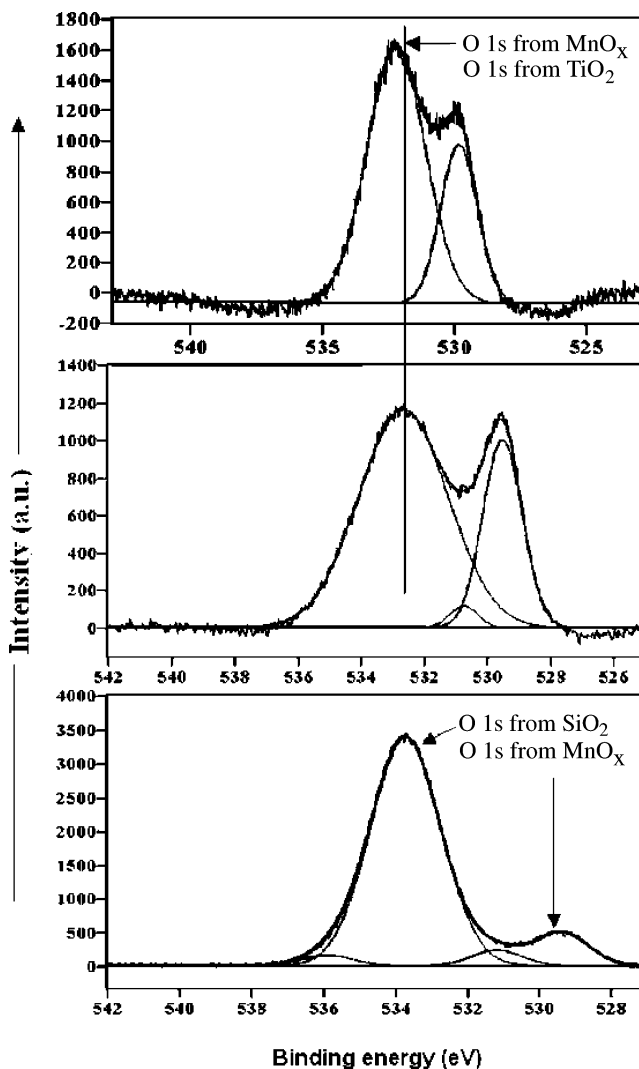
Figure 4. Deconvoluted O 1s spectra of 20 wt % Mn on different oxide supports.

and SiO$_2$ before and after the deposition of manganese oxide are shown in Figures 2 and 3, respectively. The peak intensities of the supports decreased drastically after the incorporation of manganese oxide. Here also the intensity of the XRD lines due to crystalline manganese oxide species are very low, suggesting that incorporated manganese oxide is highly dispersed on these supports and is in amorphous state.
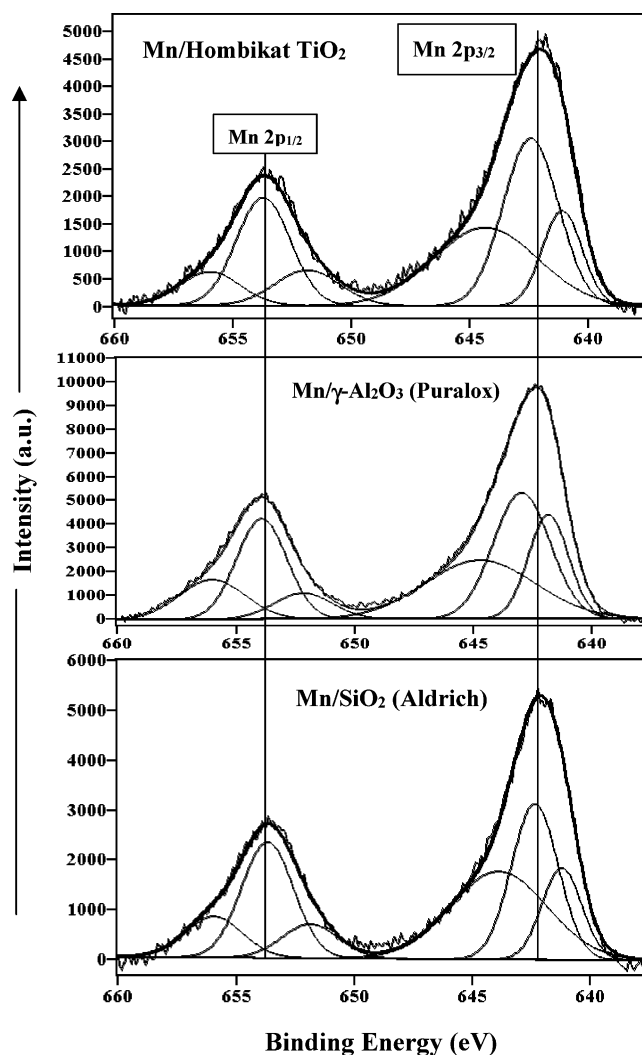
3.3. X-ray Photoelectron Spectroscopy. The deconvoluted O 1s spectra of various samples are shown in Figures 4 and 5. From Figure 4, it can be seen that all the samples show the
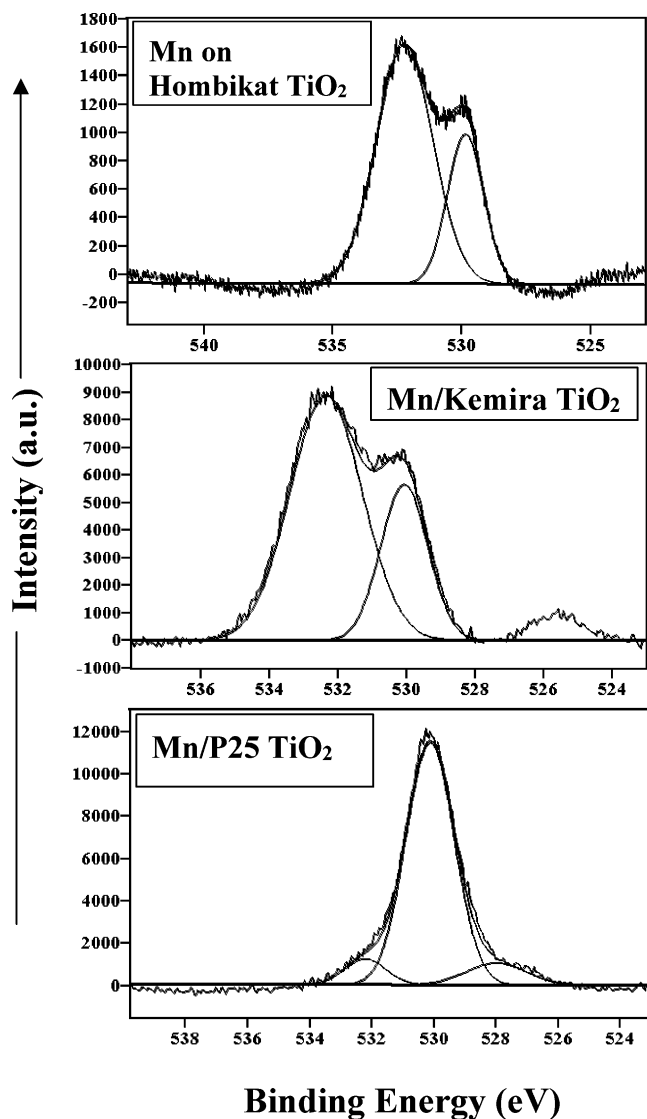
Figure 5. Deconvoluted O 1s spectra of 20 wt % Mn on different TiO$_2$ supports.

Figure 6. Deconvoluted Mn 2p spectra of 20 wt % Mn on different oxide supports.

presence of two distinct O 1s peaks, indicating that there are two different oxygen sources on the surface. In both Mn/TiO$_2$ (Hombikat) and Mn/γ-Al$_2$O$_3$ (Puralox) samples, the peak appearing at the lower binding energy value (529.3 eV) could be attributed to the oxygen from the support, while the higher binding energy peak (533.5 eV) can be attributed to oxygen from manganese oxide. The opposite trend is observed for the Mn/SiO$_2$ catalyst, where the oxygen contribution from the support appears at the higher binding energy value of 533.7 eV. Additionally, this peak is substantially larger than the peak corresponding to oxygen from manganese oxide, which is drastically different from the other two supports. This signifies that there is a substantially smaller amount of manganese on the surface of SiO$_2$ relative to the other supports. The deconvoluted O 1s spectra of different TiO$_2$-supported samples are shown in Figure 5. Oxygen originating from the manganese oxide is more predominant on the surface in the case of Hombikat and Kemira TiO$_2$-supported catalysts. However, most of the oxygen on the surface of Mn/P25 TiO$_2$ originates from TiO$_2$, as seen by the large peak at 529.8 eV.

Deconvoluted Mn 2p photoelectron spectra of various samples are shown in Figure 6. All samples show the presence of three types of photoelectron peaks with different binding energies. The largest peak at 642.4 eV and the smallest peak at 641.2 eV
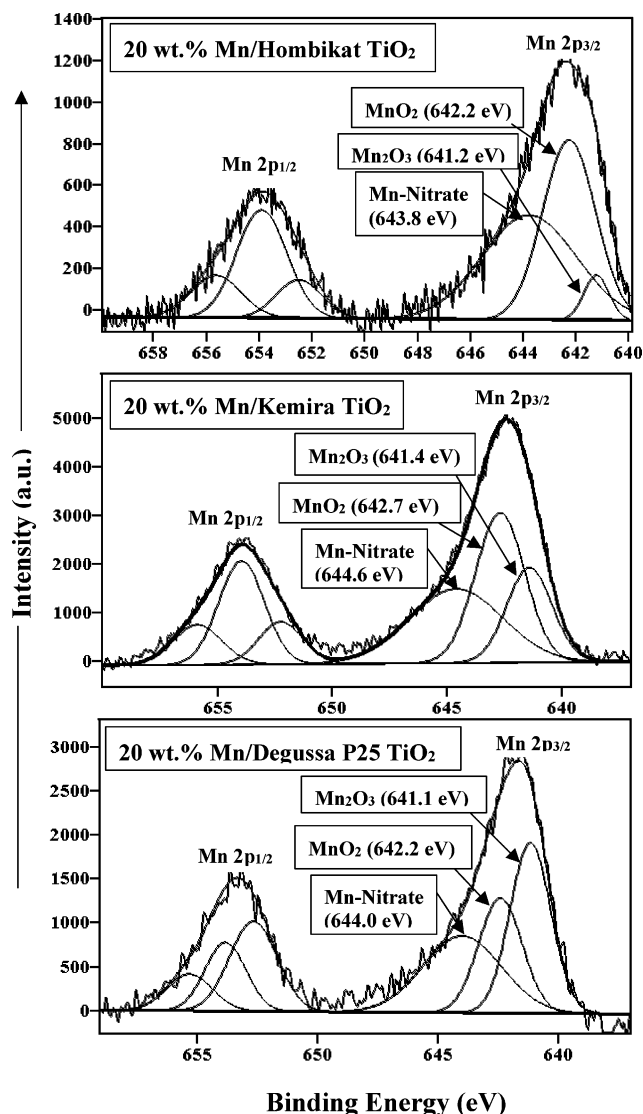
could be assigned to MnO$_2$ and Mn$_2$O$_3$ species, respectively, and agree well with the values reported in the literature.[19] The third peak at 644 eV could be assigned to partially undecomposed manganese nitrate. This peak is expected because the catalysts were calcined at a relatively low calcination temperature of 673 K. The XPS spectra of TiO$_2$ (Hombikat, Kemira, and Degussa P25) supported Mn catalysts were deconvoluted to obtain detailed information on the presence of possible metal oxide phases and their relative intensities, and these spectra are presented in Figure 7. Similar to the spectra presented in Figure 6, all three catalysts showed three deconvoluted peaks at binding energies 641.2, 642.2, and 644.5 eV corresponding to Mn$_2$O$_3$, MnO$_2$, and manganese nitrate, respectively.[19]

To confirm the presence of partially undecomposed nitrate species on the catalysts calcined at lower temperatures, an uncalcined catalyst was analyzed by XPS. A prominent peak at 644.5 eV confirmed the presence of nitrate species on uncalcined samples and the catalysts calcined at lower temperatures. Moreover, this peak disappeared for catalysts calcined at 873 K. An increased surface concentration of Mn$_2$O$_3$ for Mn supported on Kemira and Degussa (P25) TiO$_2$ catalysts can be observed in Figure 7. The confirmation of different metal oxide species with different oxidation states from XPS studies suggests a possible redox mechanism for the low-temperature SCR reaction.
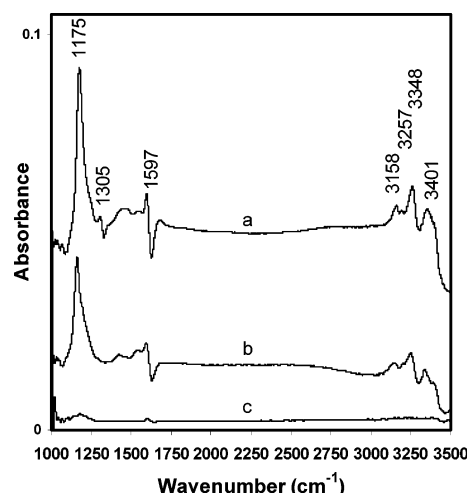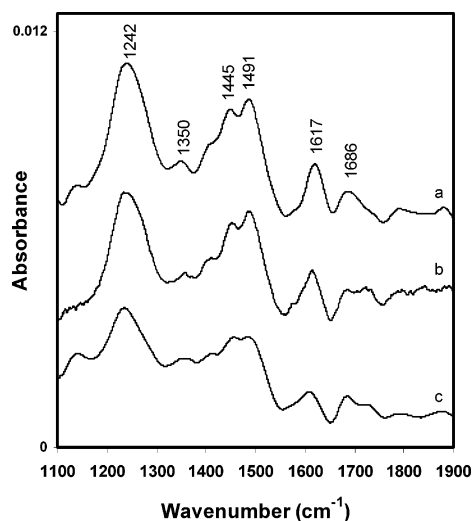
Figure 7. Deconvoluted Mn 2p spectra of 20 wt % Mn on different TiO$_2$ supports.

Figure 8. NH$_3$ FT-IR spectra collected at 323 K for 20 wt % Mn deposited on (a) TiO$_2$ (Hombikat), (b) TiO$_2$ (Degussa P25), and (c) TiO$_2$ (Aldrich).

Figure 9. NH$_3$ FT-IR spectra of 20 wt % Mn deposited on Al$_2$O$_3$ (Puralox) at (a) 323, (b) 373, and (c) 423 K.

3.4. Temperature Programmed Desorption. Ammonia TPD was utilized to measure the total acidity of the prepared catalysts and their relative acid strength. The total ammonia desorption values are presented in Table 2. All samples showed NH$_3$ desorption in the 400−700 K temperature range, signifying a broad distribution of surface acid sites. Titania-supported Mn catalysts exhibited a decrease in total acidity as surface area decreased. The amount of ammonia desorbed in the case of Mn/TiO$_2$ (Hombikat, surface area, SA, 309 m^2 g^{-1}) sample is 23.2 μmol g^{-1}, whereas the amount of ammonia desorbed in the case of Mn/TiO$_2$ (Aldrich, SA 9 m^2 g^{-1}) is 1.1 μmol g^{-1}. Among all the prepared catalysts, the Mn/γ-Al$_2$O$_3$ sample showed maximum ammonia desorption value of 31 μmol g^{-1}. The high surface area SiO$_2$-supported Mn catalyst did not show much acidity, as the total acidity was only 5.9 μmol g^{-1}. In all samples, the acid sites are distributed in two temperature regions, indicating the presence of two types of adsorbed NH$_3$ species with different thermal stabilities.

3.5. FT-IR Spectroscopy. NH$_3$ FT-IR spectra of Mn oxide deposited on various supports are presented in Figures 8−10. All the spectra were recorded under identical operating conditions and normalized. The ammonia FT-IR spectra of TiO$_2$-supported MnO$_2$ catalysts are shown in Figure 8. It is well-known in the literature that anatase TiO$_2$ adsorbs ammonia only

in the coordinated form over Lewis acid sites.[20,21] This indicates that anatase TiO$_2$ is Lewis acid, and the generation of Brönsted acid sites should be related to the Mn oxide deposited on TiO$_2$ supports. The increase of the peak intensities with an increase in support surface area was observed. The IR spectra of all three catalysts mainly show (Figure 8) the features of Lewis-bound (coordinatively adsorbed) NH$_3$ species. Surface Lewis acid sites of different strengths near 1175 cm^{-1} (strong) and 1225 cm^{-1} (weak) resulting from the splitting of the symmetric deformation mode (δ_{sym} NH$_3$, ν_2 vibrations) were seen in all three spectra, although the intensities varied. The Lewis acid peak at 1597 cm^{-1} assigned to asymmetric deformation (δ_{asym} NH$_3$, ν_4 vibrations) is less sensitive to the electronic environment of NH$_3$ molecules. In the higher wavenumber region, bands at 3158, 3257, 3348, and 3401 cm^{-1} were observed for the Mn/Hombikat TiO$_2$ catalyst. The bands are due to ν_1 and ν_3 stretching vibrations of ammonia bound to two different types of Lewis acid sites.[22,23] The weak bands at 1455 cm^{-1} (asymmetric) and 1680 cm^{-1} (symmetric) were attributed to ammonium ions and disappear once the temperature reached 373 K. Therefore, the FT-IR results suggest that the titania-supported Mn oxide catalysts are mainly Lewis acidic.

The NH$_3$ FTIR spectra of 20 wt % Mn/Al$_2$O$_3$ catalyst at 323 K is shown in Figure 9. Major IR bands from coordinated NH$_3$ species are observed in the frequency region 1600 cm^{-1}
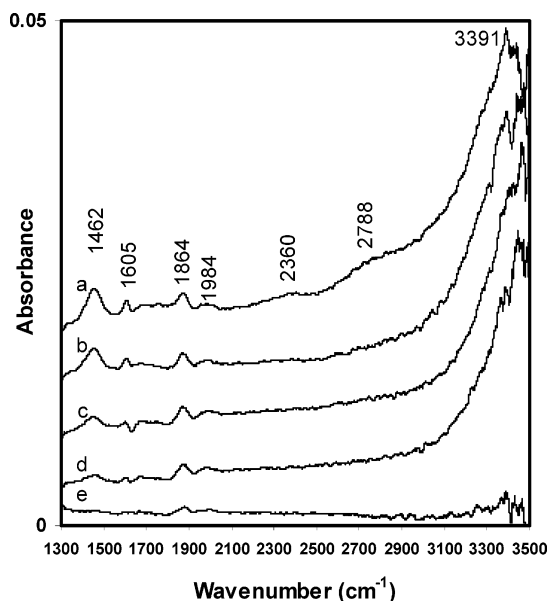
Figure 10. NH_3 FT-IR spectra collected for 20 wt % Mn deposited on SiO_2 (Aldrich) at (a) 373, (b) 423, (c) 473, (d) 573, and (e) 673 K at various temperatures.

Figure 11. H_2 TPR spectra for 20 wt % Mn deposited on (a) TiO_2 (Hombikat), (b) TiO_2 (Degussa P25), (c) TiO_2 (Aldrich), (d) Al_2O_3 (Puralox), and (e) SiO_2 (Aldrich).

(asymmetric deformation) and in the range of 1050−1330 cm^{-1} (symmetric deformation). The bands due to the ammonium ions can be observed at 1454 and 1489 cm^{-1} (asymmetric deformation) and 1680 cm^{-1} (symmetric deformation). IR bands at 1454 and 1489 cm^{-1} result from ammonia adsorption on Mn sites and Al_2O_3 sites, respectively.[24] The shoulder at 1512 cm^{-1} is due to amide species (scissoring mode), which increased slightly in intensity up to 373 K and then decreased. The spectra clearly demonstrate the interaction of ammonia with Mn/Al_2O_3 in three different ways: coordination to Lewis sites, formation of ammonium (NH_4^+) ions by the protonation of ammonia on Brönsted site, and its deprotonation leading to an amide anion. The whole process may be occurring due to the disproportionation of NH_3 as follows:

$$2NH_3 \leftrightarrow NH_4^+ + NH_2^- \qquad (1)$$

Bands from the symmetric deformation of coordinated ammonia by interaction with Lewis acid sites are found in the region 1050−1330 cm^{-1}. The bands at 1225, 1263, and 1294 cm^{-1} could be assigned to the three different Al^{3+} Lewis acid sites. These results agree well with the literature reports where three different Lewis acid sites were observed for alumina catalyst using pyridine as probe molecule.[25] The bands in the region 1100−1220 cm^{-1} and 1225−1250 cm^{-1} could be attributed to the ammonia adsorption on two different Mn^{n+} ions ($n = 3$ and 4). These results are in line with XPS results, where the presence of both MnO_2 (Mn^{4+}) and Mn_2O_3 (Mn^{3+}) has been observed.

The FT-IR spectra of Mn/SiO_2 catalyst at different temperatures are shown in Figure 10. For all the samples, main bands are observed at 1462, 1605, 1864, 1890, 2360 (broad), 2788 (broad), and 3391 cm^{-1}. It is well-known in the literature that silica is not Lewis-acidic.[26] This is mainly attributed to the difficulty in producing coordinatively unsaturated cations by condensing covalent surface hydroxyl groups. It is likely that ammonia forms hydrogen bonds with surface silanol groups, giving broad bands near 3000, 2800, and 2360 cm^{-1} and other smaller bands at 1860, 1600, 1550 (weak), and 1460 cm^{-1}. However, because of the presence of Mn oxide, the bands at 1460 cm^{-1}, and 1685 cm^{-1} may be assigned to Brönsted acid
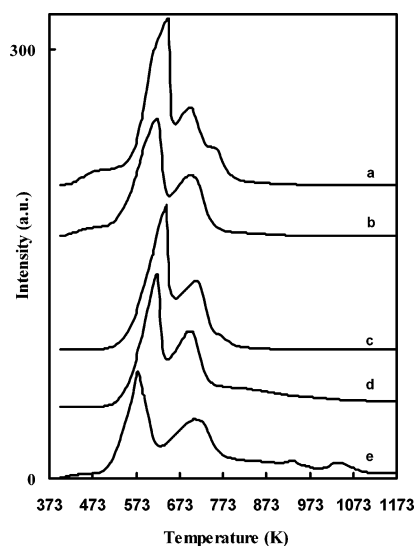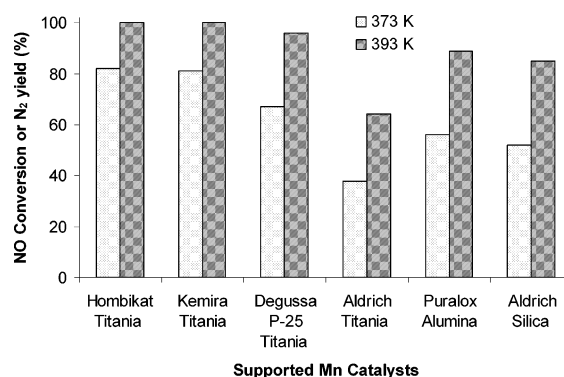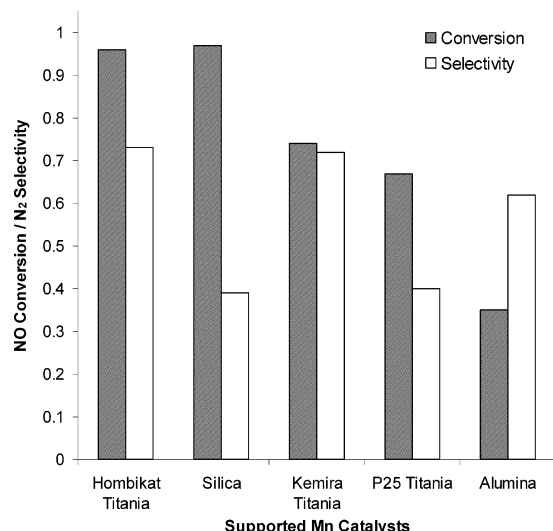

Figure 12. Catalytic activity of 20 wt % Mn on different supports for low-temperature SCR of NO with NH_3 at 373 and 393 K [NO = NH_3 = 2000 ppm, O_2 = 2.0 vol %, He balance, catalyst = 100 mg, GHSV = 8000 h^{-1}].

sites. The peak at 1605 cm^{-1} could be assigned to ammonia coordinated to Lewis acid sites.

3.6. H_2 Temperature-Programmed Reduction. The H_2 TPR profiles of various supported manganese oxide catalysts are shown in Figure 11. Figure 11 shows that a two-step reduction process was observed for all the samples. The first high intensity peak for all the samples was observed near 573−648 K, whereas the second less intense peak was found at approximately 713 K. These patterns were consistent with earlier literature reports,[27] where two distinct reduction peaks were found near 600 and 700 K for Mn/Al_2O_3 catalysts. The 20 wt % Mn/Hombikat TiO_2 catalyst also exhibits a smaller peak at 763 K. This less intense peak could be attributed to the formation of Mn_2O_3 by the reduction of MnO_2.[28] This peak was not observed in other samples, indicating the absence of the Mn_2O_3 phase. The reduction peaks at lower temperatures are due to highly dispersed MnO_x species, whereas the high-temperature peak could be due to bulk phases of manganese oxide.[28]

3.7. Catalytic Activity. The results of low-temperature SCR of NO at 373 and 393 K and at the space velocity of 8000 h^{-1} over various supported manganese oxide catalysts (20 wt % Mn) operating under identical experimental conditions are shown in Figure 12. Among the catalysts studied, Mn deposited on both Hombikat TiO_2 and Kemira TiO_2 showed superior catalytic performance over the others. Complete NO conversion with 100% N_2 selectivity was achieved at 393 K over these catalysts.

Figure 13. Catalytic activity of 20 wt % Mn on different supports for low-temperature SCR of NO with NH_3 at 448 K [NO = NH_3 = 400 ppm, O_2 = 2.0 vol %, He balance, GHSV = 50 000 h^{-1}].

The similar performance of these two supports is prominent because of their significantly different physical properties. As shown in Table 1, Hombikat TiO_2 is composed of anatase phase and possesses very high surface area (309 m^2/g) that is approximately six times greater than that of Kemira TiO_2, which is solely composed of rutile. High activity of MnO_2/Kemira TiO_2 (rutile) catalyst can be attributed to the synergistic interaction between MnO_2 and TiO_2 (R) due to the similarity in the crystalline structure, as both possess rutile crystal structure. It should be noted that a NO concentration (2000 ppm) much higher than that found in the flue gas (typically in the range of 400 ppm) of industrial power plants was used for these experiments. The performance of all the supported Mn catalysts decreased in the following order: TiO_2 (Hombikat) ≈ TiO_2 (Kemira) > TiO_2 (Degussa P25) > γ-Al_2O_3 (Puralox) > SiO_2 (Aldrich) > TiO_2 (Aldrich). With the exception of Aldrich TiO_2, which possesses an extremely low surface area, it is apparent that TiO_2 outperforms the other supports used in this study.

Since industrial SCR catalysts are used at higher gas hourly space velocities (GHSV), we investigated the activity and nitrogen selectivity of the prepared catalysts at a high space velocity of 50 000 h^{-1}, and these results are compared in Figure 13. As can be noted from this figure, significantly lower nitrogen selectivities are observed at these reaction conditions. At these conditions, the supports with the high surface area showed the highest activity. Consequently, the activity of the supported Mn catalysts tested at temperature 448 K and space velocity 50 000 h^{-1} decreased in the following order: TiO_2 (anatase) > SiO_2 > TiO_2 (rutile) > TiO_2 (anatase, rutile) > γ-Al_2O_3. Reactions carried out with 11 vol % H_2O in the feed also followed the same order. The very poor catalytic performance of Mn/Aldrich TiO_2 could be primarily attributed to the extremely low surface area of the TiO_2 support, lower surface Mn oxide concentration, and the low Lewis acidity of the catalyst. The NH_3 TPD results showed very little desorption of ammonia (1.1 μmol g^{-1}) over this catalyst relative to the other samples. The lower catalytic activity of Mn/Al_2O_3 and Mn/SiO_2 could be attributed to the dominant presence of Brönsted acid sites on these catalysts as observed in FT-IR studies.

4. Conclusions

The following conclusions can be drawn from this study.

In the XRD patterns of pure anatase and pure rutile titania-supported catalysts, crystalline MnO_2 was not observed, indicat-ing that incorporated manganese oxide is dispersed homogeneously on the supports and is in amorphous or poorly crystalline state. XPS studies indicate the presence of MnO_2 as a major phase on all the catalysts, along with Mn_2O_3 and Mn nitrate. The NH_3 FT-IR studies reveal the presence of primarily Lewis acid sites for the most active catalysts, which were TiO_2-based. Al_2O_3- and SiO_2-supported catalysts mainly possessed Brönsted acidity. Among the TiO_2-, Al_2O_3-, and SiO_2-supported manganese oxide catalysts studied for the low-temperature SCR of NO, 20 wt % Mn/TiO_2 (anatase) showed complete NO conversion and 100% N_2 selectivity at 393 K. The same catalyst also provided the highest activity and nitrogen selectivity at 448 K in the presence of 11 vol % H_2O. In conclusion, all characterization results proved that Lewis acidity, a high-surface Mn oxide concentration, and redox properties of the catalysts are important factors in achieving better DeNO$_x$ performance at low temperature.

Literature Cited

(1) Topsoe, N.-Y. Catalysis for NO$_x$ abatement. Selective catalytic reduction of NOx by ammonia: fundamentals and industrial aspects. *CATTECH* **1997**, *1*, 125.

(2) Bosch, H.; Janssen, F. Formation and control of nitrogen oxides. *Catal. Today* **1988**, *2*, 369.

(3) Lietti, L.; Svachula, J.; Forzatti, P.; Busca, G.; Ramis, G.; Bregani, F. Surface and catalytic properties of vanadia-titania and tungsten oxide-titania systems in the selective catalytic reduction of nitrogen oxides. *Catal. Today* **1993**, *17*, 131.

(4) Wood, S. C. Select the right NOx control technology. *Chem. Eng. Prog.* **1994**, *90*, 32.

(5) Dumesic, J. A.; Topsoe, N.-Y.; Topsoe, H.; Chen, Y.; Slabiak, T. Kinetics of selective catalytic reduction of nitric oxide by ammonia over vanadia/titania. *J. Catal.* **1996**, *163*, 409.

(6) Amiridis, M. D.; Wachs, I. E.; Deo, G.; Jehng, J. M.; Kim, D. S. Reactivity of V_2O_5 catalysts for the selective catalytic reduction of NO by NH_3: influence of vanadia loading, H_2O, and SO_2. *J. Catal.* **1996**, *161*, 247.

(7) Nozaki, F.; Yamazaki, K.; Inomata, T. Low temperature activity of the copper oxide catalyst supported on activated carbon for reduction of nitric oxide with ammonia. *Chem. Lett.* **1977**, 521.

(8) Singoredjo, L.; Slagt, M.; van Wees, J.; Kapteijn, F.; Moulijn, J. A. Selective catalytic reduction of NO with NH_3 over carbon supported copper catalysts. *Catal. Today* **1990**, *7*, 157.

(9) Kasaoka, S.; Sasaoka, E.; Iwasaki, H. Vanadium oxide (V_2Ox) catalysts for dry-type and simultaneous removal of sulfur oxides and nitrogen oxides with ammonia at low temperature. *Bull. Chem. Soc. Jpn.* **1989**, *62*, 1226.

(10) van der Grift, C. J. G.; Woldhuis, A. F.; Maaskant, O. L. The shell DENOX system for low temperature NO$_x$ removal. *Catal. Today* **1996**, *27*, 23.

(11) Zhu, Z.; Liu, Z.; Liu, S.; Niu, H.; Hu, T.; Liu, T.; Xie, Y. NO reduction with NH_3 over an activated carbon-supported copper oxide catalysts at low temperatures. *Appl. Catal., B* **2000**, *26*, 25.

(12) Yoshikawa, M.; Yasutake, A.; Mochida, I. Low-temperature selective catalytic reduction of NO$_x$ by metal oxides supported on active carbon fibers. *Appl. Catal., A* **1998**, *173*, 239.

(13) Blanco, J.; Avila, P.; Suárez, S.; Martín, J. A.; Knapp, C. Alumina-and titania-based monolithic catalysts for low temperature selective catalytic reduction of nitrogen oxides. *Appl. Catal., B* **2000**, *28*, 235.

(14) Curry-Hyde, H. E.; Musch, H.; Baiker, A. Selective catalytic reduction of nitric oxide over amorphous and crystalline chromia: I. Comparative study of activities. *Appl. Catal.* **1990**, *65*, 211.

(15) Schneider, H.; Maciejewski, M.; Köhler, K.; Wokaun, A.; Baiker, A. Chromia supported on titania: VI. Properties of different chromium oxide phases in the catalytic reduction of NO by NH_3 studied by *in situ* diffuse reflectance FTIR spectroscopy. *J. Catal.* **1995**, *157*, 312.

(16) Singoredjo, L.; Korver, R.; Kapteijn, F.; Mouljin, J. Alumina supported manganese oxides for the low-temperature selective catalytic reduction of nitric oxide with ammonia. *Appl., Catal. B* **1992**, *1*, 297.

(17) Smirniotis, P. G.; Peña, D. A.; Uphade, B. S. Low temperature selective catalytic reduction (SCR) of NO with NH_3 by using Mn, Cr and Cu oxides supported on Hombicat TiO_2. *Angew. Chem., Int. Ed.* **2001**, *40*, 2479.

(18) Peña, D. A.; Uphade, B. S.; Smirniotis, P. G. TiO_2-supported metal oxide catalysts for low-temperature selective catalytic reduction of NO with NH_3: I. Evaluation and characterization of first row transition metals. *J. Catal*. **2004**, *221*, 421.

(19) Kapteijn, F.; Dick van Langeveld A.; Moulijn, J. A.; Andreini, A.; Vuurman, M. A.; Turek, A. M.; Jehng, A. M.; Wachs, I. E. Alumina-supported manganese oxide catalysts: I. Characterization: effect of precursor and loading. *J. Catal*. **1994**, *150*, 94.

(20) Hino, M.; Mikami, Y. Infrared spectra of ammonia adsorbed on titanium dioxide. *Bull. Chem. Soc. Jpn*. **1983**, *56*, 3495.

(21) Amores, J. M. G.; Escribano, V. S.; Ramis, G.; Busca, G. An FT-IR study of ammonia adsorption and oxidation over anatase-supported metal oxides. *Appl. Catal., B* **1997**, *13*, 45.

(22) Primet, M.; Pichet, P.; Mathieu, M. V. Infrared study of the surface of titanium oxides. 1. Hydroxyl groups. *J. Phys. Chem*. **1971**, *75*, 1216.

(23) Dines, T. J.; Rochester, C. H.; Ward, A. M. Infrared and Raman study of the adsorption of NH_3, pyridine, NO and NO_2 on anatase. *J. Chem. Soc., Faraday. Trans*. **1991**, *87*, 643.

(24) Kapteijn, F.; Singoredjo, L.; van Driel, M.; Andreïni, A.; Moulijn, J. A.; Ramis, G.; Busca, G. Alumina supported manganese oxide catalysts: II. Surface characterization and adsorption of ammonia and nitric oxide. *J. Catal*. **1994**, *150*, 105.

(25) Knözinger, H. Specific poisoning and characterization of catalytically active oxide surfaces. *Adv. Catal*. **1976**, *25*, 184.

(26) Odenbrand, C. U. I.; Brandin, J. G. M.; Busca, G. Surface acidity of silica-titania mixed oxides. *J. Catal*. **1992**, *135*, 505.

(27) Singoredjo, L.; Korver, R.; Kapteijn, F.; Moulijn, J. Alumina supported manganese oxides for the low-temperature selective catalytic reduction of nitric oxide with ammonia. *Appl. Catal., B* **1992**, *1*, 297.

(28) Liu, Y.; Luo, M.; Wei, Z.; Xin, Q.; Ying, P.; Li, C. Catalytic oxidation of chlorobenzene on supported manganese oxide catalysts. *Appl. Catal., B* **2001**, *29*, 61.